BIOCHEMISTRY
including biophysical chemistry & molecular biology

Article

A spectroscopic study on the aggregation state of the human antimicrobial peptide LL-37 in bacterial versus host cell model membranes

Alessio Bonucci, Elena Caldaroni, Enrico Balducci, and Rebecca Pogni

Biochemistry, **Just Accepted Manuscript** • DOI: 10.1021/acs.biochem.5b00813 • Publication Date (Web): 26 Oct 2015

ACS Publications

Biochemistry is published by the American Chemical Society. 1155 Sixteenth Street N.W., Washington, DC 20036

A spectroscopic study on the aggregation state of the human antimicrobial peptide LL-37 in bacterial *versus* host cell model membranes

Alessio Bonucci [a], *Elena Caldaroni* [a], *Enrico Balducci* [b] *and Rebecca Pogni* [a*]

[a]Department of Biotechnology, Chemistry and Pharmacy, University of Siena, 53100 Siena, Italy

[b]School of Biosciences and Medicine Veterinary, University of Camerino, Camerino, Italy

ABSTRACT

The LL-37 antimicrobial peptide is the only cathelicidin peptide found in humans that has antimicrobial and immunomodulatory properties. Since it exerts also chemotactic and angiogenetic activity, LL-37 is involved in promoting wound healing, reducing inflammation and increasing the host immune response. The key to the effectiveness of Anti Microbial Peptides (AMPs) lies in the different composition of bacterial versus host cell membranes. In this context the antimicrobial peptide LL-37 and two variants were studied in the presence of model membranes with different lipid compositions and charges. The investigation has been performed using an experimental strategy which combines the Site Directed Spin Labeling-Electron Paramagnetic Resonance (SDSL-EPR) technique with Circular Dichroism and Fluorescence emission spectroscopies. LL-37 interacts with negative charged membranes forming a stable aggregate, which can likely originate toroidal pores until the amount of bound peptide exceeds a critical concentration. At the same time we have clearly detected an aggregate with a higher oligomeric degree for interaction of LL-37 with neutral membrane. These data confirm the absence of cell selectivity of the peptide and a more complex role in stimulating host cells.

INTRODUCTION

With the rapid increase of antibiotic-resistant bacterial strains, the discovery of therapeutic agents with a different mode of action is growing of importance. Antimicrobial Peptides (AMPs) represent a suitable alternative for a new generation of antibiotics[1-3]. Peptides in this class are characterized by common features: they are cationic and amphipathic, suggesting that their mechanism of action is related, to a great extent, on the different lipid composition of bacterial versus host cell membranes[4-6]. The latter are prevalently formed by the zwitterionic lipid phosphatidylcholine (POPC) and cholesterol, which impart to membrane a neutral charge and some degree of rigidity[7-9]. The difference between Gram-positive and Gram-negative bacteria resides mainly on the lipopolysaccharides composition of their cell walls[10]. In contrast, the cytoplasmic membranes of Gram-negative bacteria are prevalently composed by phosphatidylethanolamine (POPE) and, to a lesser extent, by phosphatidylglycerol (POPG) and cardiolipin (CL) conferring the membrane a net negative charge[11,12].

LL-37, the only human cathelicidin, is released by proteases from its precursor hCAP-18 (i.e. human cationic antimicrobial protein, ~18 kDa) and is an effector of the innate immune system[13]. This peptide has been extensively studied for its properties as a host defense peptide and its role in human health is now firmly established, i.e LL-37 concentration is strongly reduced in airways of cystic fibrosis patients[14]. LL-37 has a net charge of +6 at neutral pH and a random coil conformation in aqueous solution that is replaced by an helical secondary structure and self-assembling into oligomers under physiological salt conditions and in the presence of model membranes[15-19]. Differently from other antimicrobial peptides, LL-37 at concentrations greater than Minimal Inhibitory Concentration (MIC = 5 μM) exhibits also cytotoxic activity towards host cells[16]. In attempts to describe the mechanism underlying the peptide antimicrobial

activity, a toroidal pore mechanism was inferred from solid state NMR experiments on oriented bilayers, in contrast with a non-pore carpet mechanism reported previously[17,20].

To obtain a deeper insight on the different behavior towards the interaction of LL-37 with bacterial versus host cell membranes, Large Unilamellar Vesicles (LUVs) with lipid composition resembling that of bacterial-like (POPE:POPG:CL 70:25:5) versus mammalian-like membrane (POPC:POPE:Chol:CL 55:15:25:5)[8], have been used to analyze the LL-37 lipid partitioning at different peptide to lipid molar ratios. With this aim, a SDSL-EPR spectroscopic approach has been performed with the combined use of Circular Dichroism and fluorescence emission spectroscopies. Two different LL-37 variants, LL-37 F27W where a Trp replaces Phe27 and LL-37 L28C where a Cys replaces Leu28, were used to perform the Fluorescence and SDSL-EPR analysis respectively. Our results indicate that the antimicrobial peptide LL-37 interacts with the bacterial-like membranes in the form of a stable aggregate, which, at increasing membrane bound peptide, can likely originate toroidal pores. An aggregate form, characterized by a higher degree of oligomerization has clearly been detected with neutral membranes. This aspect reveals a moderate selectivity of this peptide, which once self-aggregated can modulate either the antimicrobial activity and host cell modulating effect[18].

EXPERIMENTAL PROCEDURES

Materials

The LL-37 peptide was obtained from Bachem (Bubendorf, CH) and the LL-37 F27W and LL-37 L28C variants were obtained from China peptides (Shanghai, RC) and used without further purification (**Figure 1A**).

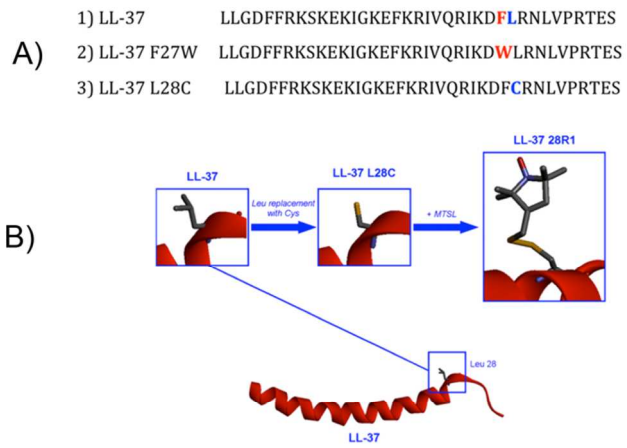

Figure 1. (A) Aminoacidic sequences of native LL-37, LL-37 F27W and LL-37 L28C variants. In blue and red colours the positions 27 and 28 are highlighted. (B) Spin-labeling reaction scheme of LL-37 L28C variant with the MTSL spin probe. The LL-37 spin labeled peptide (LL-37 L28R1) structure was obtained with *Visual Molecular Dynamics* and *Discovery Studio* tools (LL-37 2K6O pdb code)[21].

The phospholipids for vesicles preparation, 1-palmitoyl-2oleoyl-sn-glycerol-3-phosphoglycerol (POPG), 1-palmitoyl-2oleoyl-sn-glycerol-3-phosphoethanolamine (POPE), 1-palmitoyl-2oleoyl-sn-glycerol-3-phosphocholine (POPC), 1,1',2,2'-tetramyristoyl cardiolipin ammonium salt (CL), spin-labeled phosphatidylcholine (1-acyl-2-[n-(4,4dimethyloxazolidinyl-N-oxyl)]stearoyl-sn-glycero-3-phosphocholine, n-PCSL, with n= 5,7,12) and cholesterol were obtained from Avanti Polar Lipids (Alabaster, AL). The methanethiosulfonate spin label, MTSL (1-oxy-2,2,5,5-tetramethylpyrroline-3-methyl methanethiosulfonate) was obtained from Toronto Research Chemicals Inc. (Toronto,CDN). The buffer solution (pH 6.8) contains 50 mM of 3-(N-morpholino) propanesulfonic acid (MOPS) (Sigma Aldrich). MOPS is a buffer largely used for biological sample preparation with a 0.025M ionic strength[22].

Liposome Preparation

Liposomes mimicking the lipid composition of the Gram-negative inner bacterial

membrane and an average composition of eukaryotic membrane were prepared mixing the specific phospholipids (POPE:POPG:CL 70:25:5 molar ratios) and (POPC:POPE:Chol:CL 55:15:25:5 molar ratios) respectively[23]. The stock concentration of relative phospholipids and sterol used for bacterial and mammalian model membranes were: POPE 14 mM, POPG 12.9 mM CL 6.6 mM, POPC 14 mM and Chol 50 mM.

For the preparation of both types of model membranes, lipids at the desired molar ratio were dried down from chloroform stock solutions under a stream of nitrogen gas and then dried under vacuum for 1h. The resulting lipid film was hydrated by adding 50 mM MOPS at pH 6.8 for a final concentration of about 50 mM phospholipids. Large unilamellar vesicles (LUVs) were prepared by freeze-thawing this lipid suspension five times followed by extrusion through 200 nm polycarbonate membrane filters using a mini-extruder syringe device (Avanti Polar Lipids). Final concentration of LUVs was determined using the Stewart phospholipids assay[24]. LUVs containing 1 mol of 5, 7, or 12-PCSL were prepared as described above. The spin label in the phospholipid acyl chain at 5, 7 and 12 positions allows to monitor distances from the surface of the bilayer approximately equal to 7.5Å, 8.1Å and 13.2Å respectively[25].

Circular Dichroism

Circular Dichroism (CD) experiments were performed at room temperature on a Jasco CD-J-815 spectropolarimeter using a quartz cuvette with a path length of 1 mm. Native LL-37 peptide (0.03 mM) was dissolved in 50 mM MOPS at pH 6.8 and was incubated with vesicular suspension ranging from 0.15 to 7.5 mM concentration. LL-37 F27W and L28C variants were dissolved in MOPS solution. The CD spectra showed the same secondary structure of the wild type peptide (data not shown). A mixed solution, 50% trifluoroethanol (TFE) and 50% (v/v) MOPS at pH = 6.7 was used to check folding and aggregation state of the wild type and spin-

labeled variant in presence of the isotropic helix-promoting solvent.

Each CD spectrum was recorded from 190 to 250 nm at room temperature and was accumulated at least ten times to improve the signal-to-noise ratio. Baselines of either solvent or membranes solution without peptide were subtracted from the respective sample spectra to calculate the peptide contribution[26]. The quantitative analysis of the CD spectra was performed using the freely available program "DICHROWEB" (Birkbeck, London College)[27].

Fluorescence spectroscopy

The replacement of Phe27 with the aromatic residues Trp in the LL-37 F27W variant was performed to insert a strong fluorophore into the aminoacidic sequence without altering the hydrophobicity of the peptide (**Figure 1A**). The former substitution was chosen as the 17-29 fragment of the peptide facilitates the insertion of LL-37 in the lipid membranes[15]. Furthermore the replacement of Phe27 with a Trp residue introduces a minimal perturbation to the peptide sequence and does not affect the antimicrobial activity[28]. Samples prepared for fluorescence measurements contained 0.04 mM peptide and a variable phospholipid concentration ranging from 0.2 to 10 mM. Fluorescence measurements were performed on a Jasco FB-6500 spectrometer. The excitation wavelength was 280 nm, and emission spectra were recorded between 290 and 420 nm, with a 1 nm slit widths at room temperature[29,30].

Spin Labeling and EPR spectroscopy

To perform the Site Directed Spin Labeling EPR (SDSL-EPR) study, the LL-37 L28C variant (**Figure 1A**) was used. The presence of a cysteine residue was required for the binding of the radical probe. Since the spin label side chain is relatively hydrophobic, normally a leucine

is a conservative substitution. The substitution of a leucine (e.g. Leu28) with a cysteine residue does not induce any specific structural change in the peptide and does not affect the LL-37 interaction with liposomes[31].

LL-37 L28C was initially dissolved in the buffer for the spin labeling reaction (50mM MOPS, 100mM NaCl, 2mM $MgCl_2$, pH 6.8). Subsequently, a 5-fold molar excess of MTSL was added to the sample, which was placed on a plate with stirring at 4°C overnight in the absence of light to avoid unwanted secondary reactions. LL-37 spin labeled peptide (LL-37 L28R1) (**Figure 1B**) was initially dialyzed with MWCO 2 kDa benzoylated tube (Sigma-Aldrich) in spin buffer solution for 24h at 4°C to partially remove the excess of non-reacted MTSL. The solution was purified with a desalting column (5mL Hi-Trap desalting, GE Healthcare) attached to an AKTA-FPLC to completely remove the unreacted nitroxide radical. Spin labeled peptide was concentrated using 3kDa Amicon-Ultra device (Millipore) and the final concentration was evaluated by UV-Vis analysis (Molar extinction coefficient ε = 780.4 cm^{-1} M^{-1}). The EPR spectrum of the spin labeled variant (LL-37 L28R1) was recorded to check the absence of free MTSL from the peptide solution[31].

The EPR spectra of the spin labeled peptide were recorded on a Bruker E500 ELEXSYS X-Band spectrometer equipped with a super-high-Q cavity. Samples prepared for EPR measurements contained 0.04 mM of peptide and a variable concentration of LUVs ranging from 0.2 mM to 10 mM. Spectra were recorded using the following instrumental settings: 120 G sweep width; 100 kHz modulation frequency; 1.0 G modulation amplitude; 40 ms time constant at; 20 mW microwave power. Several scans, generally 20, were run to improve the signal-to-noise ratio.

The Multi-Component EPR program

(http://www.biochemistry.ucla.edu/biochem/Faculty/Hubbell/) was used to simulate the EPR spectra; this program is a fitting platform for nitroxide CW-EPR spectral lineshape to calculate an EPR spectrum as a function of input parameters.

To analyze the LL-37 insertion into bacterial model membrane, LUVs containing 1mol % of 5-, 7- or 12 PCSL were prepared and the EPR spectra were recorded. The relative values of $2\Delta A_{max}$ were obtained by calculating the difference of outer hyperfine splitting constant for the spectra in presence or absence of LL-37. To assess the rotational mobility of 12-PCSL, the apparent rotational correlation time (τ) was determined according to (eq. 1):

$$\tau = (0.65\times10^{-9})\,\Delta H_0\,[(A_0/A_{-1})^{1/2} - 1] \qquad (1)$$

where ΔH_0 is the peak-to-peak width of the center line in gauss, A_0 is the amplitude of the center line and A_{-1} is the amplitude of high field line (see refs. 31-32 for more details). The rotational correlation time is inversely related to the motional spin label rate such that an increase in τ indicates a slower motion.

RESULTS

Circular Dichroism and Fluorescence analysis

In **Figure 2A** (*open circles*) the CD spectrum of free peptide in buffer solution (50 mM MOPS, pH = 6.8) is reported. The spectrum shows a typical random coil conformation characterized by a negative band at 198 nm. The use of a buffer at low ionic strength allows the peptide to be in an unordered conformation differently from other buffer at high ionic strength where the peptide takes an helical arrangement[18,19]. Indeed, adding LUVs (model bacterial membrane) at 1:250 peptide:lipid molar ratio a variation in CD lineshape is observed (**Figure 2A** ***down triangles***). In this condition, LL-37

shows a mixed secondary structure characterized by the coexistence of the peptide in a random coil (~ 82%) and α-helix (~ 18%) arrangements due to the presence of bands at 200 nm, 210 nm and 220 nm. At higher ratios (1:50 and 1:20, **Figure 2A *up triangles* and *squares*** respectively) a well-defined CD spectra of the peptide in its α-helical form (~ 92%) indicates a complete folding of LL-37. For 1:5 peptide: lipid molar ratio (**Figure 2A *solid circles***) peaks at ~210 nm and ~220 nm are still present.

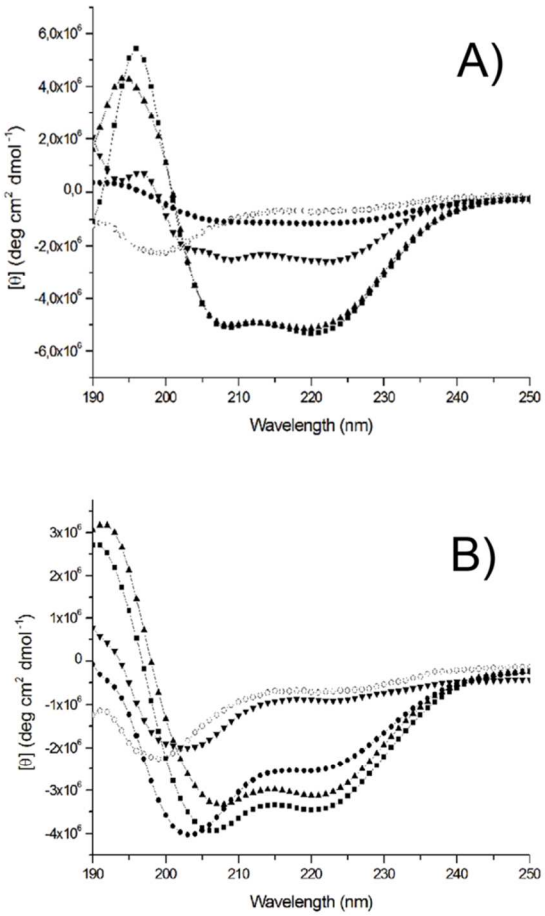

Figure 2. (A) CD spectra of native LL-37 in 50 mM MOPS buffer (*open circles* in A and B panels) and with POPE:POPG:CL and (B) POPC:POPE:Chol:CL membranes. Each spectrum was collected at room temperature ten times to reduce signal to noise ratio. Peptide:lipid molar ratios were: 1:250 (*down triangles*), 1:50 (*up triangles*), 1:20 (*squares*) and 1:5 (*solid circles*).

A similar analysis has been performed for LL-37 in solution and with model eukaryotic

membranes (POPC:POPE:Chol:CL). No particular differences were observed when lipids were added at 1:250 peptide:lipid molar ratio (**Figure 2B *down triangles***) compared to the free form of LL-37 in MOPS, only a small amount of α-helix secondary structure is detected (~10%). For 1:50 and 1:20 ratios (**Figure 2B *up triangles and squares*** respectively), CD spectra display double absorbance peaks at 210 nm and 220 nm with a lineshape indicating an α-helical secondary structure (~70% and 80% respectively). For the 1:5 peptide:lipid molar ratio (**Figure 2B *solid circles***) a more pronounced negative band at 204 nm is detected revealing that a part of LL-37 is still unfolded for this ratio (~90%). The CD results show that for zwitterionic membranes the helical structure of LL-37 peptide is in equilibrium with its unstructured form.

Tryptophan fluorescence emission represents a useful method to investigate the interaction of peptides with lipid membranes. The blue shift and the increase in quantum yield of fluorescence emission band are the main features observed when a Trp moves from water to an apolar environment[35,36]. Since LL-37, in its native form, does not contain any fluorophore, the LL-37 F27W variant was used for this spectroscopic analysis.

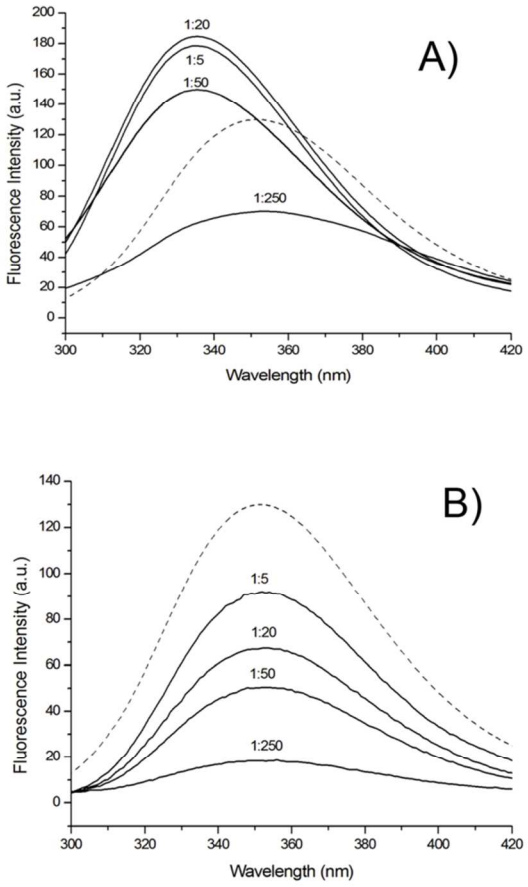

Figure 3. (A) Fluorescence emission spectra of LL-37 F27W variant in solution (*dotted* line, A and B panels) and in the presence of POPE:POPG:CL and (B) POPC:POPE:Chol:CL membranes. Spectra were recorded with an excitation wavelength of 280 nm at room temperature. Each spectrum was collected three times to reduce signal-noise ratio.

In **Figure 3A** the tryptophan emission spectra of LL-37 F27W with or without POPE:POPG:CL LUVs at different molar ratios are reported. Free peptide in MOPS buffer (**Figure 3A *dotted line***) displays a fluorescence band at 352 nm, indicating a solvent exposed Trp residue. To the highest LUVs concentration (1:250 peptide:lipid) no changes of the emission band but a reduction in the fluorescence quantum yield was recorded. Furthermore at this ratio the fluorescence emission is quite low due to the light scattering effect of the high LUVs concentration. At 1:50, 1:20 and 1:5 peptide:lipid molar ratios a blue shift of the emission band at 336 nm and an increase in the fluorescence quantum yield were

observed for all the conditions tested. These results revealed that increasing membrane bound peptide (decreasing peptide:lipid molar ratio), LL-37 binds to the lipid bilayer, with the Trp experiencing a less polar environment.

The same experiments were performed in the presence of POPC:POPE:CL:Chol LUVs (**Figure 3B**). At all peptide:lipid ratios, no blue shift of the emission band was recorded evidencing that Trp did not monitor the hydrophobic core of lipid bilayer.

Binding and mobility of the spin-labeled peptide

Site Directed Spin Labeling (SDSL) gives information on local structure and environment and is well suited to study the dynamics and aggregation state of small peptides in solution and in a membrane environment[37-39]. It is based on the attachment of a nitroxide radical probe to the thiol group of a cysteine residue of the protein aminoacidic sequence. The continuous wave EPR spectra reflecting the motion of the spin probe can be used to evaluate the partitioning of peptides in the presence of different amounts of lipid dispersion. The variant of the LL-37 (LL-37 L28C, **Figure 1B**), was spin labeled with MTSL (see Experimental Procedures) and was then used to further explore peptide-membrane interactions with the two types of model membranes.

EPR spectra of spin labeled LL-37 L28R1 in MOPS buffer and in 50% TFE / 50% (v/v) MOPS are shown in **Figure 4A** and **4C** respectively.

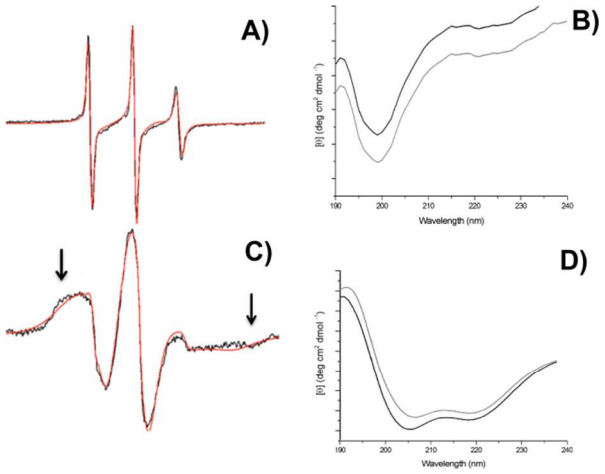

Figure 4. (A) Experimental (*black line*) and simulated (*red line*) CW-EPR spectra of LL-37 L28R1 variant. (B) CD spectra of native LL-37 (*grey line*) and LL-37 L28R1 variant (*black line*). (C) Experimental (*black line*) and simulated (*red line*) CW-EPR spectra of LL-37 L28R1 variant. D) CD spectra of LL-37 L28R1 (*black line*) and LL-37 (*grey line*). For EPR and CD spectra reported in panels A) and B) a 50 mM MOPS buffer at pH 6.8 was used, while for the EPR and CD spectra reported in panels C) and D) a mixed solution 50% TFE/50% MOPS at pH = 6.7 was used. EPR and CD data were collected 10 times to increase the signal/noise ratio.

The spin labeled peptide in buffer solution (**Figure 4A *black line***) displays an EPR spectrum composed by three narrow lines, typical of a fast tumbling motion of the radical probe. In the absence of spin exchange, the EPR spectra reflect the dynamic effects of the spin label as well as that of the reorientation of the peptide. The sharp lines of the spectrum reported in **Figure 4A** (paired with its simulation, **Figure 4A *red line***) indicate rapid isotropic motion indicative of the spin label in a random coil structure with a 0.43 ns correlation time. These results are consistent with the CD data where the peptide is in a random coil arrangement (**Figure 4B *grey* and *black lines***). When a mixed solution of TFE (50% TFE/50% MOPS) is used, an intensity decrease with a broadening of the spectrum components is detected (Fig. **4C)**. This indicates the existence of a species with higher correlation time (slower motion) where the lines in the EPR spectrum are broadened by spin-spin interactions[40] (**Figure 4C *black line***). A more detailed analysis of the EPR spectrum reported in **Figure 4C** shows at least two spin populations with different motional mobility both of them derived from different protein

aggregation states (the arrows in **Figure 4C** highlight the aggregation state with a higher degree of oligomerization). A small percentage of monomer (a contribution from the spectrum reported in Fig. 4A) can also be identified. The comparison of the EPR spectrum of LL-37 L28R1 in MOPS solution to that in 50% TFE/50% MOPS, underlines an overall decrease in the rotational freedom of the spin label suggesting that the helix formation and peptide aggregation are concerted processes in this isotropic solvent. In **Figure 4D** the CD spectra are consistent with the formation of an helical secondary structure.

To probe the partitioning of LL-37 in the highly directional membrane environment, the spin labeled peptide was incubated with POPE:POPG:CL LUVs at different peptide:lipid molar ratios. In **Figure 5A** the EPR spectra are reported.

In the presence of liposomes, intensity decreases and broadening of the lines is observed indicating a reduction in spin label mobility upon membrane binding for all the tested ratios. The correlation time for this species is equal to 4.3 ns. The appearance of the same lineshape for all the peptide:lipid ratios and the absence of a sharp component in the EPR spectra due to the unstructured, unbound peptides, underlines that the spin labeled peptides are fully bound in a stable aggregated state to the negatively-charged membranes.

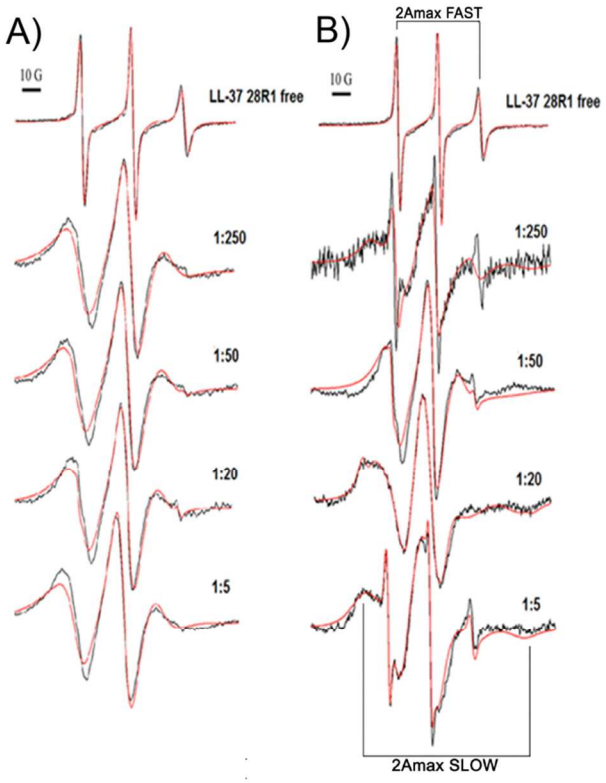

Figure 5. (A) Experimental (*black line*) and simulated (*red line*) CW-EPR spectra of LL-37 L28R1 in 50 mM MOPS buffer at pH 6.8, in the presence of POPE:POPG:CL and (B) POPC:POPE:Chol:CL model lipid membranes. $2A_{max}$ for the fast and slow tumbling motion of the spin probe is marked.

The same analysis has been performed also with neutral lipid bilayer (POPC:POPE:Chol:CL) that mimics an average composition of mammalian membranes (**Figure 5B**). The presence of cholesterol changes the state of the bilayer toward a local ordered state (L_0), conferring to these membranes some degrees of rigidity[9]. It is interesting to note that, differently from bacterial membranes, all the EPR spectra are composed by at least two superposed spin populations with different motional mobility due to the equilibrium between the bound (aggregate) and unbound (unordered-monomeric) peptide. The oligomeric and monomeric species are characterized by different rotational correlation times, which are reported in Table 1. For 1:250 pep:lip, the contribution due to the slow motion spectrum (bound peptide) is reduced compared to the unbound form (free peptide), indicating that only a small percentage of peptide is bound to the bilayer (~ 16% from EPR simulation).

This is in agreement with the CD spectrum (**Figure 2A *down triangles***) where only 18% of the peptide is in its helical arrangement. Increasing the membrane-bound peptide (1:50 molar ratio) the slow motion spectrum of the nitroxyl radical overcomes the fast motion one, while the aggregate state is similar to that detected in bacterial membranes with an estimated correlation time of ~ 4.0 ns. Decreasing LUVs concentration (1:20) two different spin populations with a rotational correlation time equal to 4.00 ns (~ 64%) and 4.45 ns (~ 36%) are detected respectively. This indicates two species with different peptide aggregation states. The aggregate with the higher degree of oligomerization and slower motion (higher correlation time) is well defined for the 1:5 peptide:lipid molar ratio. At this ratio the presence of ~ 20% of the fast motion species, due to the unbound monomeric peptide, points out an equilibrium between the aggregate state and the free form of the peptide. This trend shows that LL-37 interacts in oligomeric forms with mammalian–like membranes suggesting a reduced selectivity of LL-37 and likely a more complex physiological role.

Table 1. Correlation times of slow and fast motion components for the spin labeled peptide (LL-37 28R1[a]) in MOPS pH=6.8, in the presence of [b]bacterial like and [c]mammalian-like model membranes

	Slow Motion $\tau \pm 0.08$ (nsec)	Fast Motion $\tau \pm 0.08$ (nsec)
[a] LL-37 28R1 free	–	0.43
[b] POPE:POPG:CL	4.00	–
[c] POPC:POPE:Chol:CL	4.00 and 4.45	0.36

Correlation times have been calculated with Multi-Component EPR simulation program (see Experimental Procedures)

Effect of LL-37 binding on bacterial-like membranes

The EPR technique has been used to analyze the insertion of peptides into LUVs using site-specific spin labeled lipids. To determine the lipid penetration of LL-37, the motion of phosphatidylcholine with a nitroxide radical positioned at different depths on the alkyl chain is examined. Changes in the outer hyperfine coupling constant ($2A_{max}$) of the EPR spectrum reflect the selectivity of interaction with lipid head-groups and also the different strengths of lipid interaction with peptides[31,32,41-43]. Based on fluorescence results, experiments on peptide penetration into the phospholipid bilayer using spin labeled lipids have been performed only for bacterial-like membranes.

In **Figure 6** (***squares***) and **Table 1** the differences on outer hyperfine splitting constants in the presence and in the absence of peptide ($2\Delta A_{max}$) for membranes containing 5-PCSL lipid are reported. For 1:250 peptide:lipid molar ratio LL-37 presents a small values of $2\Delta A_{max}$ indicating no significant perturbation of membrane surface. For the other conditions (1:50, 1:20 and 1:5 peptide:lipid molar ratios) almost the same values of $2\Delta A_{max}$ have been obtained suggesting a slight decrease in motion (i.e. an increase in $2\Delta A_{max)}$ with increasing bound peptide (**Figure 6** *squares* **and Table 1**). The same trend has also been reported for 7-PCSL (**Figure 6** ***circles*** **and Table 1**).

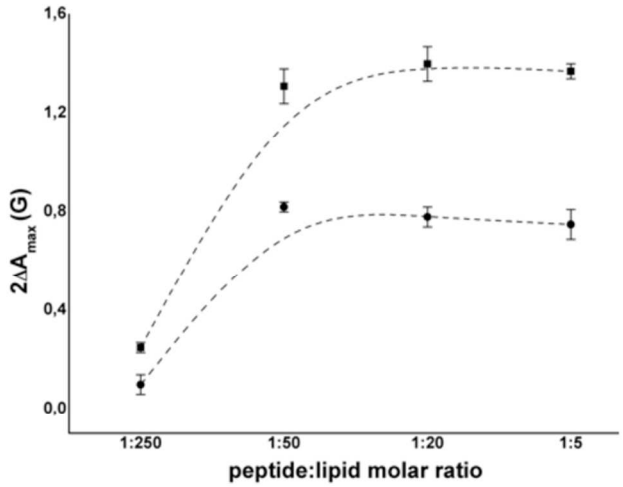

Figure 6. Variation of $2\Delta A_{max}$ for different LL-37:LUVs molar ratios calculated for 5- (*squares*) and 7-PCSL (*circles*). Error bars indicate standard deviation from three independent measurements.

Table 2. Differences in outer hyperfine splittings ($2\Delta A_{max}$) for 5-PCSL and 7-PCSL, incorporated in model bacterial LUVs (POPE:POPG:CL) at different peptide:lipid molar ratios

	5-PCSL	7-PCSL
pep:lip	$2\Delta A_{max}$ ±0.06G	$2\Delta A_{max}$ ± 0.07G
1:250	0.21	0.12
1:50	1.31	0.75
1:20	1.39	0.71
1:5	1.37	0.68

The mean standard errors (±) of the differences in outer splitting constants have been calculated from three independent measurements

As 12-PCSL undergoes more rapid motion than 5- or 7-PCSL, the width of the central line (ΔH_0) or relative line amplitudes, can be used to calculate the empirical rotational correlation time (see Eq. 1 and Table 3). Overall these results indicate that the perturbation of bilayer lipid motional dynamics upon accumulation of bound LL-37 is observed only near the membrane surface. Furthermore, we have to take into account that the formation of oligomeric forms, sequestering the spin label inside the oligomer might also be responsible for the low variation on the motional parameters for 12-PCSL.

Table 3. Motional parameters for 12-PCSL incorporated in model bacterial LUVs (POPE:POPG:CL) as a function of peptide:lipid molar ratios.

pep:lip	[a]$\Delta H_0 \pm 0.05$G	[b]$\tau \pm 0.06$ nsec
0:1	3.91	3.31
1:250	3.81	3.38
1:50	3.94	3.75
1:20	4.01	3.87
1:5	4.01	3.84

The mean standard errors (±) of the [a]peak-to-peak width of the central line and [b]correlation time have been calculated from three independent measurements

DISCUSSION

LL-37 is the only antimicrobial peptide belonging to the human cathelicidin family. It is stored in neutrophils along with α-defensins and constitutes one of the first lines of defence against infection in human organisms[13,44]. LL-37 has attracted considerable interest as possible candidate to replace common antibiotics, since it possesses a broad spectrum of activity against microorganisms and can be obtained easily by chemical synthesis[15].

The lipid partition of LL-37 was characterized in different single phospholipid monolayers, bilayers and binary mixtures of phospholipids, showing that for LL-37 the lipid head-group charge does not play a dominant role in determining the mode of lipid-protein interaction[45]. Again, on the basis of a solid state NMR study of oriented bilayers, it was shown that the α-helix lies parallel to the surface of lipid bilayers and a toroidal pore model of bilayer disruption was inferred[20]. In contrast, a detergent-like effect via a carpet-like mechanism was proposed as the mode of action of LL-37 with negatively-charged membranes[17]. Previous investigations have shown that the helical conformation of LL-37 is

charge, pH and concentration dependent and that the extent of helical content is related to its antibacterial activity[16]. The high content of anionic and cationic charges in the peptide sequence favors helix conformation and aggregation state with the formation of intra- and inter-molecular salt bridges in the presence of physiological salt concentrations and membrane-like environments[17-19]. In this paper we have studied the dynamic and aggregation state of LL-37 in buffer solution, in the presence of the helix-promoting solvent TFE (TFE/MOPS) and with bacterial-like versus mammalian-like membranes. The peptide has been analyzed at a concentration higher than MIC (5 μM against *E. coli* D21)[16] and at different peptide:lipid molar ratios. The use of MOPS, a buffer with a low ionic strength, allows the peptide to be in a monomeric (unfolded) structure in bulk solution, differently from other buffers at high ionic strength, which favor peptide aggregation[19]. The spin labeling technique allows to investigate specific domains of the secondary structure. This technique also gives information on different peptide aggregation states through the determination of the correlation times i.e. fast motion means low correlation times. In this context the EPR spectrum of LL-37 L28R1 in MOPS at pH = 6.8 shows that the peptide is in its monomeric unfolded form, while the presence of more than one spin populations in TFE/MOPS solution, characterized by different rotational correlation times, are evident (Fig. 4A and C). In this case the formation of helical secondary structure (as evidenced by the CD spectrum, Fig. 4D) is accompanied by the formation of different oligomerization states of the peptide.

The main features of the lipid bilayer of eukaryotic cell membrane are: the presence of cholesterol (10-25%) and the large amount of zwitterionic phosphatidylcholine lipids (POPC) that confers neutral charge to the outer leaflet. In contrast, bacterial inner membranes are prevalently constituted by zwitterionic phosphatidylethanolamine (POPE) and by 20-25% of negatively charged lipids, such as phosphatidylglycerol (POPG) and cardiolipin (CL)[8-12]. The presence of POPG, in bacterial membranes, should govern the membrane partitioning of LL-37 through electrostatic interactions between the

negative polar heads of phospholipids and the cationic residues of peptides. In contrast, the presence of cholesterol in mammalian bilayer, determines an increase in the order and membrane rigidity lowering the peptide partitioning[46].

Bacterial-like membrane model

The EPR spectra reported in Figure 6 show that LL-37 L28R1 binds to the bacterial membrane in a well-defined oligomeric form with a correlation time of 4.00 ns (Table 1). The oligomeric form remains stable increasing the membrane bound peptide (decreasing LUVs concentration).

On the other hand the blue shift of the fluorescence emission band, starting from 1:50 peptide:lipid molar ratio, shows that the fluorophore moves from a polar to an apolar environment. The small variation in the empirical rotational correlation time collected for 12-PCSL bacterial membrane do not give a clear evidence for a membrane spanning mode of the peptide as it was clearly stated for α-defensin once the peptide threshold concentration was reached[47].

Our data state that LL-37 is self-associated as an oligomer on the anionic membrane. The mechanism through which the peptide remains parallel to the membrane surface until overcoming a peptide threshold concentration and then inserts into the hydrophobic core with a likely toroidal pore formation cannot be ruled out[19]. The sequestering of spin label inside the peptide oligomeric form could likely be the reason why no clear evidence for a deeper insertion of the peptide into the lipid bilayer was detected.

Mammalian-like membrane model

A different peptide behavior has been revealed for zwitterionic liposomes. The peptide, at the lowest molar ratio (1:250), is partially bound (~10% helical structure) to the lipid bilayer, no evident

changes in the secondary structure are recorded compared to the free form. Only for the 1:20 and 1:50 peptide:lipid molar ratios the CD spectra showed a high content of α-helical structure for LL-37 interaction with the neutral membranes (~70-80%).

Paired to this, no shift variation on the fluorescence emission band is detected at all the tested peptide:lipid molar ratios. This may indicate no partition of the fluorophore into the bilayer hydrophobic core. At the same time, the increase in the emission quantum yield, moving from 1:250 to 1:5 molar ratio can be related to a decrease in tryptophan self-quenching due to the dissociation of associated peptides in the presence of neutral membranes. The EPR data show the most interesting results when LL-37 is incubated with zwitterionic LUVs. Spin populations with different mobility are present as the concentration of membrane-bound peptide increase (from 1:250 to 1:5 molar ratios) with changes in the aggregate/monomer equilibrium. The EPR spectra reported in **Figure 5B** show that the monomer (fast motion component, not bound peptide) is always in equilibrium with different oligomeric states of the peptide (slow motion component, bound peptide) and once reached the 1:5 molar ratio the aggregate state with the higher rotational correlation time (τ = 4.45 ns, higher degree of oligomerization) is in equilibrium with its monomeric form. The formation of an aggregate species with a higher oligomeric degree in neutral membrane is in agreement with previous results[48]. This might correlate with the stimulatory effect of LL-37 on host cells, since the aggregated form stimulate fibroblast proliferation through the $P2X_7$ receptor[48].

In vivo, LL-37 shows a cooperative antibacterial activity with defensins against microorganism infections in humans[44]. In our previous work, we investigated the mechanism of action of Human Neutrophil Peptide 1 (HNP-1) using the same model bacterial membranes used in the present study and a membrane spanning-mode mechanism at a threshold concentration equal to 1:20 peptide:lipid molar

ratio was inferred[47]. The positive charge of AMPs drives the electrostatic interaction with anionic phosphate head groups while the non-polar residues determine the penetration into the bulk of lipid bilayer. LL-37 presents a +6 cationic charge at physiological pH with a GRAVY index of -0.72 compared to HNP-1 that shows a +3 charge and a GRAVY index of 0.30[49]. HNP-1 is mainly hydrophobic and inserts deeply into the hydrophobic core of the membrane. Instead, LL-37 interacts with the membrane with both electrostatic and hydrophobic effects. It interacts as aggregated species on the lipid headgroups, aligned on the surface of the bilayer partially penetrating into the hydrophobic core of bacterial-like membranes. The particular arrangement of the cationic and anionic charges in the peptide sequence determines the mode of interaction of LL-37 with neutral membranes where the peptide sits in an extended aggregation state. The oligomeric form drives the multifaced activity of LL-37 not only for the antimicrobial activity against the anionic membrane but also towards the host cells.

These results point out that the lipid composition of the membranes affects the interaction and insertion of LL-37 into the bilayer influencing also the oligomerization state.

CONCLUSIONS

In conclusion, LL-37 is present as an unfolded monomeric peptide in MOPS buffer (τ_C = 0.43 ns) while in a mixed solution (50% TFE/50% MOPS) at physiological pH is self-associated in helical aggregates. This suggests that the adoption of the secondary structure is concomitant with the formation of the oligomeric state. In the presence of negatively-charged bacterial membranes LL-37 forms a stable aggregate (τ_C = 4.0 ns), which likely, increasing the membrane-bound peptide, forms toroidal pores enhancing vesicle permeability. The different lipid composition of the mammalian-like membranes induces the formation of a more extended oligomerization state of the peptide (τ_C = 4.45 ns). These data have shown that LL-37 is not as selective as some other α-helical amphipathic

antimicrobial peptides and this is consistent with the formation of the oligomeric state in the presence of neutral membranes confirming the absence of cell selectivity of this peptide.

Corresponding Author

* Prof. Rebecca Pogni, PhD

Department of Biotechnology, Chemistry and Pharmacy

University of Siena

Via A. Moro 2

53100 Siena, Italy

e-mail: rebecca.pogni@unisi.it

Tel. +39 0577 234258

ABBREVIATIONS

AMP, antimicrobial peptide; CD, Circular Dichroism; Chol, cholesterol; CL, 1,1',2,2'-tetramyristoyl cardiolipin ammonium salt; CW-EPR, Continous Wave Electron Paramagnetic Resonance; GRAVY, Grand Average Hydropathicity; LUV, Large Unilamellar Vesicle; MOPS, 3-(N-morpholino) propanesulfonic acid; MTSL, methan thiosulphonate spin label; PCSL, phosphatidylcholine spin-labels; POPC, 1-palmitoyl-2-oleoyl-sn-glycero-3-phosphocholine; POPE, 1-palmitoyl-2-oleoyl-sn-glycerol-3-phosphatidylethanolamine, POPG, 1-palmitoyl-2-

oleoyl-sn-glycerol-3-phosphatidylglycerol; POPS, 1-hexadecanoyl-2-(9Z-octadecenoyl)-sn-glycero-3-phospho-L-serine sodium salt; SDSL, Site Directed Spin Labeling;

ACKNOWLEDGEMENTS

The CSGI (Consorzio Interuniversitario per lo sviluppo dei Sistemi a Grande Interfase) is gratefully acknowledged.

REFERENCES

1. Boman, H.G. (1995) Peptide antibiotics and their role in innate immune, *Annu. Rev. Immunol 13,* 61-92.

2. Zalstoff, M. (2002) Antimicrobial peptides of multicellular organism, *Nature 415,* 389-395.

3. Hancock, R.E.W., and Chapple, D.S. (1999) Peptide antibiotics, *Antimicrob. Agents Chemother. 43,* 1317-1323.

4. Brodgen. K.A. (2005) Antimicrobial peptides: pore former or metabolic inhibitors in bacteria? *Nat. Rev. Microbiol. 3,* 238-250.

5. Reddy, K.V.R., Yedery, R.D., and Aranha, C. (2004) Antimicrobial peptides. Premises and promises, *Int. J. Antimicrob. Agents 24,* 536-547.

6. Yeman, M.R., and Yount, N.Y. (2003) Mechanism of antimicrobial peptide: action and resistance, *Pharmacol. Rev. 55,* 27-54.

7. Van Meer, G., Voelker, D.R., and Feigenson, G.W. (2008) Membrane lipids: where they are and how they behave, *Nat. Rev. 9,* 112-124.

8. Van Meer, G., and de Kroon, A.I.P.M. (2011) Lipid map of the mammalian cell, *J. Cell. Sci. 124,* 5-8.

9. Vitiello, G., Fragneto, G., Petruk, A.A., Falanga, A., Galdiero, S., D'Ursi A.M., Merlino, A. and D'Errico, G. (2013) Cholesterol modulates the fusogenic activity of a membranotropic domain of the FIV glycoprotein gp36, *Soft Matter 9,* 6442-6456.

10. D'Errico, G., Silipo, A., Mangiapia, G., Vitiello, G., Radulescu, A., Molinaro, A., Lanzetta, R. and Paduano, L. (2010) Characterization of liposomes formed by lipopolysaccharides from *Burkholderia cenocepacia, Burkholderia multivorans* and *Agrobacterium tumefaciens*: from the molecular structure to the aggregate architecture, *Phys. Chem. Chem. Phys. 12,* 13574-13585.

11. Cronan, J.E. (2003) Bacterial membrane lipids: where do we stand?, *Ann. Rev. Microbiol. 57,* 203-224.

12. Lopes, S., Neves, C.S., Eaton, P., and Gameiro, P. (2010) Cardiolipin, a key component to mimic the E.coli bacterial membrane in model system revealed by dynamic light scattering and steady-state fluorescence anisotropy, *Anal. Bioanal. Chem. 398,* 1357-1366.

13. Vandamme, D., Landuyt, B., and Schoofs, L. (2012) A comprehensive summary of LL-37, the factotum human cathelicidin peptide, *Cell. Immunol. 280,* 22-35.

14. Bals, R., Weiner, D.J., Meegella, R.L., and Wilson, J.M. (1999) Transfer of cathelidin peptide antibiotic gene restores bacterial killing in cystic fibrosis xenograft model, *J. Clin. Invest. 103,* 1113-1117.

15. Porcelli, F., Verardi, R., Shi, L., Henzler-Wildman, K.A., Ramamoorthy A. and Veglia G. (2008) NMR structure of the cathelicidin-derived human antimicrobial peptide LL-37 in dodecylphosphocholine micelles, *Biochemistry 47,* 5565-5572.

16. Johansson, J., Gudmundsson, G.H., Rottenberg, M.E., Berndt, K.D., and Agerberth, B. (1998) Conformation-dependent antibacterial activity of the naturally occurring human peptide LL-37, *J. Biol. Chem. 273,* 3718-3724.

17. Oren, Z., Lerman, J.C., Gudmundsson, G.H., Agerberth, B., and Shai, Y. (1999) Structure and organization of the human antimicrobial peptide LL-37 in phospholipid membranes: relevance of the molecular basis for its non-cell selective activity, *Biochem. J. 341,* 501-513.

18. Xhindoli, D., Pacor, S., Giuda, F., Antcheva, N., and Tossi, A. (2014) Native oligomerization determines the mode of action and biological activities of human cathelicidin LL-37, *Biochem. J. 457,* 263-275.

19. Xhindoli, D., Morgera, F., Zinth, U., Rizzo, R., Pacor, S., and Tossi, A. (2015) New aspects

of the structure and mode of action of the human cathelicidin LL-37 revealed by the intrinsic probe p-cyanophenylalanine *Biochem. J. 465,* 443-457.

20. Henzler Wildman, K.A., Lee, D.K., and Ramamoorthy, A. (2003) Mechanism of lipid bilayer disruption by the human antimicrobial peptide LL-37, *Biochemistry 42,* 6545-6558.

21. Wang, G. (2008) Structures of human host defense cathelicidin LL-37 and its smallest antimicrobial peptide KR-12 in lipid micelles, *J. Biol. Chem. 283,* 32637-32643.

22. Good, N.E., Winget, G.D., Winter, W., and Connolly, T.N. (1966) Hydrogen ion buffers for biological research, *Biochemistry 5,* 467-477.

23. Epand, R. M., and Epand, R.F. (2003) Liposomes as models for antimicrobial peptides, *Methods Enzymol. 372,* 124-133.

24. Stewart, J.C.M. (1980) Colorimetric determination of phospholipids with ammonium ferrothiocynate, *Anal. Biochem. 104,* 10-14.

25. Kyrychenko, A. and Ladokhin, A.S. (2013) Molecular Dynamics simulations of depth distribution of spin-labeled phospholipids within lipid bilayer, *J. Phys. Chem. B 117,* 5875-5885.

26. Heller, W.T., Waring, A.J., Lehrer R.I., and Huang, H.W. (1998) Multiple states of beta – sheet peptide protegrin in lipid bilayers, *Biochemistry 37,* 17331-17338.

27. Lobley, A., Whitmore, L. and Wallace, B.A. (2002) DICHROWEB: an interactive website for the analysis of protein secondary structure from circular dichroism spectra, *Bioinformatics 18,* 211-212.

28. Sood, R., Domanov, Y., Pietiäinen, M., Kontinen, V.P., and Kinnunen, P.K.J. (2008) Binding of LL-37 to model membranes: Insight into target vs host cell recognition, *Biochim. Biophys. Acta 1778,* 983-986.

29. Ladokhin, A.S., Jayasinghe S., and White, S.H. (2000) How to measure and analyze

tryptophan fluorescence in membrane properly, and why bother?, *Anal. Biochem. 285,* 235-245.

30. Christianes, B, Symoens, S., Vanderheyden, S., Englborghs, Y., Joliot, A., and Prochiants, A., Vandekerckhove, J., Rosseneu M. and B. Vanloo, (2002) Tryptophan fluorescence study of the interaction of penetrating peptides with model membranes, *Eur. J. Biochem. 269,* 2918-2926.

31. Pistolesi, S., Pogni, R., and Feix, J.B. (2007) Membrane insertion and bilayer perturbation by antimicrobial peptide CM15, *Biophys. J. 93,* 1651-1660.

32. Bonucci, A., Balducci, E., Martinelli, M., and Pogni, (2014) R. Human neutrophil peptide 1 bearing modified arginine cationic side chain: effects on membrane partitioning, *Biophys. Chem. 190-191,* 32-40.

33. Lee, C.C., Sun, Y., Qian, S., and Huang, H.W. (2011) Transmembrane pores formed by human antimicrobial peptide LL-37, *Biophys J. 100,* 1688-1696.

34. Thennarasu, S., Tan, A., Penumatchu, R., Shelburne, C.E., Heyl, D.L., and Ramamoorthy, A. (2010) Antimicrobial and membrane disrupting activities of a peptide derived from the human cathelicidin antimicrobial peptide LL-37, *Biophys. J. 98,* 248-257.

35. Ladokhin, A.S., Jayasinghe, S., and White, S.H. (2000) How to measure and analyse tryptophan fluorescence in membrane properly, and why bother?, *Anal. Biochem. 285,* 235-245.

36. Christianes, B. Symones, S., Vanderheyden, S., Englborghs, Y., Joliot, A., Prochiants, A., Vandekerckhove, J., Rosseneu, M. and Vanloo, B. (2002) Tryptophan fluorescence study of the interaction of penetrating peptides with model membranes, *Eur. J. Biochem. 269,* 2918-2926.

37. Bhrgava, K., and J.B. Feix, (2002) Membrane binding, structure and localization of cecropin-mellitin hybrid peptides: a site-directed spin-labeling study, *Biophys. J. 86,* 329-336.

38. Hubbell, W.L., and Altenbach, C. (1994) Investigation on structure and dynamics in membrane proteins using site-directed spin labeling, *Curr. Opin. Struct. Biol. 4,* 566-573.

39. Frazier, A.A., Roller, C.R., Havelka, J.J., Hinderliter, A., and Cafiso, D.S. (2003) Membrane-bound orientation and position of the synaptotagmin I C2A domain by site-directed spin labeling, *Biochemistry 42,* 96-105.

40. Mchaourab, H.S., Hyde, J.S., and Feix, J.B. (1993) Aggregation state of Spin-Labeled Cecropin AD in Solution, *Biochemistry 32,* 11895-11902.

41. Pistolesi, S., Rossini, L., Ferro, E., Basosi, R., Trabalzini, L., and Pogni, R. (2009) Humanin structural versatility and interaction with model cerebral cortex membrane, *Biochemistry 48,* 5026-5033.

42. D'Errico, G., D'Ursi, A.M., and Marsh, D. (2008) Interaction of a peptide derived from glycoprotein gp36 of feline immunodeficiency virus and its lipoylated analogue with phospholipid membranes, *Biochemistry 47,* 5317-5327.

43. Ramakrishnan, M., Jensen, P.H., and Marsh, D. (2003) α-Synuclein association with posphatidylglycerol probed by lipid spin labels, *Biochemistry 42,* 12919-12926.

44. Nagaoka, I., Hirota, S., Yomogida, S., Ohwada, A., and Hirata, M. (2000) Synergistic actions of antibacterial neutrophil defensins and cathelicidins, *Inflamm. Res. 49,* 73-79.

45. Sevcsik, E., Pabst, G., Richter, W., Danner, S., Amenitsch, H., and Lohner, K. (2008) Interaction of LL-37 with model membrane systems of different complexity: influence of lipid matrix, *Biophys. J. 94,* 4688-4699

46. Brender, J.R., McHenry, A.J., and Ramamoorthy, A. (2012) Does cholesterol play a role in bacterial selectivity of antimicrobial peptides?, *Front. Immunol. 3,* 1-4.

47. Bonucci, A., Balducci, E., Pistolesi, S., and Pogni, R. (2013) The defensin-lipid interaction: insights on the binding states of the human antimicrobial peptide HNP-1 to model bacterial membranes, *Biochim. Biophys. Acta 1828,* 758-764.

48. Tomasinsig, L., Pizzirani, C., Skerlavaj, B., Pellegatti, P., Gulinelli, S., Tossi, A., Di Virgilio, F. and Zanetti, M. (2008) The Human Cathelicidin LL-37 modulates the activities of the P2X7 receptor in a structure- dependent manner, *J. Biol. Chem. 283,* 30471-30481.

49. Kyte, J. and Doolittle, R.F. (1982) A simple method for displaying the hydrophathic character of protein, *J. Mol. Biol. 157,* 105-132.

TOC